Thermal and dielectric properties of PEO/EC/Pr$_4$N$^+$I$^-$ polymer electrolytes for possible applications in photo-electro chemical solar cells

T. M. W. J. Bandara · B.-E. Mellander · I. Albinsson · M. A. K. L. Dissanayake · H. M. J. C. Pitawala

Abstract The anion-conducting polymer electrolyte polyethylene oxide (PEO)/ethylene carbonate (EC)/Pr$_4$N$^+$I$^-$/I$_2$ is a candidate material for fabricating photo-electrochemical (PEC) solar cells. Relatively high ionic conductivity values are obtained for the plasticized electrolytes; at room temperature, the conductivity increases from 7.6×10^{-9} to 9.5×10^{-5} S cm^{-1} when the amount of EC plasticizer increases from 0% to 50% by weight. An abrupt conductivity enhancement occurs at the melting of the polymer; above the melting temperature, the conductivity can reach values of the order of 10^{-3} S cm^{-1}. The melting temperature decreases from 66.1 to 45.1 °C when the EC mass fraction is increased from 0% to 50%, and there is a corresponding reduction in the glass transition temperature from −57.6 to −70.9 °C with the incorporation of the plasticizer. The static dielectric constant values, ε_s', increase with the mass fraction of plasticizer, from 3.3 for the unplasticized sample to 17.5 for the 50% EC sample. The dielectric results show only small traces of ion-pair relaxations, indicating that the amount of ion association is low. Thus, the iodide ion is well dissociated, and despite its large size and relatively low concentration in these samples, the iodide ion to ether oxygen ratio is 1:68, a relatively efficient charge carrier. A further enhancement of the ionic conductivity, especially at lower temperatures, is however desired for these applications.

Keywords PEC solar cells · Polymer electrolyte · Ionic conductivity · Dielectric properties

T. M. W. J. Bandara · M. A. K. L. Dissanayake ·
H. M. J. C. Pitawala
Department of Physics and Postgraduate Institute of Science,
University of Peradeniya,
Peradeniya, Sri Lanka

T. M. W. J. Bandara
Department of Physical Sciences,
Rajarata University of Sri Lanka,
Mihintale, Sri Lanka

T. M. W. J. Bandara (✉) · B.-E. Mellander
Department of Applied Physics,
Chalmers University of Technology,
Göteborg, Sweden
e-mail: awijendr@yahoo.com

I. Albinsson
Department of Physics, University of Gothenburg,
Göteborg, Sweden

Introduction

Solid polymer electrolytes are emerging as potential materials for the development of solid state batteries [1–3], photo-electrochemical (PEC) solar cells [4–6], electrochromic devices, and fuel cells due to the increased demand for these devices in the last two decades [7]. However, most of the research work on polymer electrolytes has been aimed at improving cationic conductivity and other properties due to their possible applications in secondary lithium ion batteries. Comparatively little work has been reported on solid polymer electrolytes intended to be used as anionic conductors for PEC solar cells [4–6].

A widely used redox couple for TiO$_2$ based dye-sensitized solar cells is the I$_3^-$/I$^-$ system [4–6, 8]. It has been used in aqueous/organic solutions or gel or solid polymer electrolytes. The incorporation of iodine is needed to facilitate the redox reaction [9–11] because I$_3^-$ is formed associating I$^-$ and I$_2$. It has also been reported that the incorporation of iodine increases the conductivity of the electrolyte [11]. Most of the liquid or gel or solid polymer electrolytes have used a molar ratio of 10:1 or 10:2 for salt

to iodine [6, 9, 10, 12]. It is also reported that ionic liquids intended for PEC solar cells have given the best results for 100:1 salt to I_2 weight ratio [13]. The role of the I^-/I_3^- redox couple in PEC solar cell applications is discussed in detail in references [9, 10, 12]. In this study, we selected to use 10:1 salt to iodine molar ratio, which was also used in our previous work on PEC solar cell fabrication. The gel and solid electrolyte forms are more promising, as they can prevent leakage problems and also improve long term stability. In addition, there are also other technological advantages such as the flexibility of the geometry of the electrolyte membranes and the chemical inertness of the host polymer toward the electrodes. Energy conversion efficiencies of about 3–5% have been reported for TiO_2-based dye-sensitized solar cells containing gel or solid polymer electrolytes with the I_3^-/I^- redox couple [4, 12, 14]. The reported room temperature conductivities of such electrolytes have reached values of the order of 10^{-3}–10^{-5} S cm^{-1}. These values have been achieved by incorporating plasticizers such as ethylene carbonate (EC), propylene carbonate (PC), or polyethylene glycol (PEG) or by forming composites with ceramic fillers like fumed silica [4, 6, 12, 15].

Polyethylene oxide (PEO) is a semi-crystalline solid with a relatively high degree of crystallinity at room temperature. The ionic conductivity in PEO-salt electrolytes occurs mainly in the amorphous elastomeric phase due to segmental motion and inter- and intra-atomic hopping mechanisms [16]. The magnitude of the ionic migration basically depends on the free charge carrier concentration, temperature, and dynamics of the host matrix and also on the inter-ionic interactions. Furthermore, cross-linking involving polymer, plasticizer, and ionic species also affect the conductivity and mechanical properties of the electrolyte. The crystallinity of PEO inhibits the ionic mobility and reduces the ionic conductivity. It is well known that the crystallinity of PEO can be reduced by incorporating plasticizers with relatively high dielectric constants, like EC or PC, thus improving conductivity [2]. To our knowledge, there are no reports on the study of dielectric behavior of electrolytes to be used in PEC solar cells, although there are several reports available on the dielectric properties of Li$^+$ ion conducting solid polymer electrolytes. In a previous paper, we reported the iodide ion conductivity of a PEO-based, solid polymer electrolyte incorporating the tetrapropylammonium iodide ($Pr_4N^+I^-$) and its application in a PEC solar cell [8]. The present work is aimed at establishing the inter-relationships and correlation between thermal and electric data in order to better understand these materials for further development. In this paper, we report the thermal, electrical, and dielectric properties of solid polymer electrolyte membranes with PEO to salt weight ratio of 9:1 optimized for the highest conductivity.

Experimental

PEO (M_w, 4,000,000), $Pr_4N^+I^-$, iodine chips (I_2), and EC, all with purity greater than 98% purchased from Aldrich were used as starting materials. PEO and $Pr_4N^+I^-$ were vacuum-dried for 24 h in a vacuum oven at 50 °C prior to use. For the preparation of the electrolyte samples, the weights of $Pr_4N^+I^-$ (0.065 g), I_2 (0.005 g), and PEO (0.63 g) were kept unchanged in order to obtain an electrolyte with composition $(PEO)_{68}Pr_4N^+I^-/I_2$, and the weight of EC was varied. The samples were prepared using the solvent casting method. The selected compositions of chemicals were dissolved in anhydrous acetonitrile solvent (30 ml) and were magnetically stirred at room temperature for 24 h, until a homogeneous viscous solution was obtained. The resulting slurry was cast on to a Teflon plate and kept inside a fume box for 24 h in order to gradually drive off the solvent. This procedure yielded visually homogeneous polymer electrolyte films, which were vacuum-dried for 24 h prior to measurements in order to study the variation of ionic conductivity with temperature. The low frequency complex impedance measurements were performed using a Schlumberger SI-1260 impedance-gain phase analyzer in the frequency range of 10 Hz–10 MHz and in the temperature range of 30 to 100 °C in a temperature regulated oven (Buchi—Model TO-50). Disc-shaped electrolyte films of diameter 13 mm and thickness 0.1–0.4 mm, sandwiched between two polished stainless steel blocking electrodes, were used for impedance measurements.

High-frequency complex impedance measurements were performed using a HP 4291 A RF impedance analyzer in the frequency range 1 MHz–1GHz and in the temperature range of 20 to 80 °C. A flow of nitrogen gas was maintained over the sample holder to prevent contact with atmospheric moisture. In order to obtain dielectric data, disc-shaped electrolyte films of diameter 5 mm and thickness 0.1–0.4 mm were sandwiched between two polished stainless steel blocking electrodes and AC-impedance measurements were taken.

The thermal properties of the samples were analyzed using a Mettler Toledo DSC 30 differential scanning calorimeter from −120 to 120 °C in the heating cycle, with a heating rate of 10 °C min^{-1}.

Results and discussion

The ionic conductivity (σ) of the $(PEO)_{68}Pr_4N^+I^-/I_2$/EC-based polymer electrolytes for different EC concentrations are shown in Fig. 1 as a function of inverse temperature. In general, the conductivity increases with increasing mass fraction of plasticizer, although at higher temperatures, the 16.7% EC sample shows the lowest conductivity. The

Fig. 1 The conductivity versus 1,000/T for (PEO)$_{68}$Pr4N$^+$I$^-$/I$_2$/EC electrolytes containing different mass fractions of EC
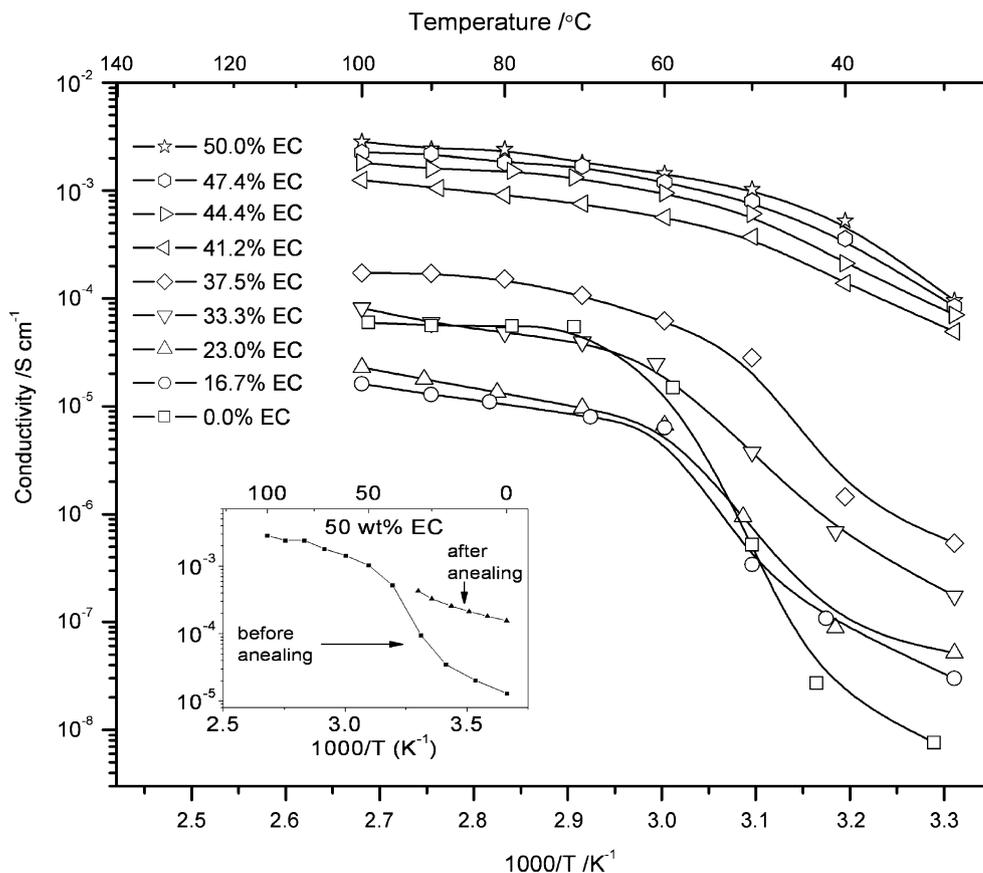
highest conductivity for all temperatures is obtained for the sample with the highest EC mass fraction of 50%. The curves for EC concentrations higher than 40% show high conductivity and Vogel–Tamman–Fulcher-like behavior. For lower EC content, a distinct increase in the ionic conductivity is observed when the temperature passes through the polymer melting temperature. However, the conductivity above this temperature is still considerably lower than for the samples with high EC content. The distinct increase in conductivity is also observed in an extended measurement shown in the inset in Fig. 1 and for the 50% EC sample. At high temperatures, above ~60 °C, the curves are relatively linear, and in order to facilitate the analysis, a fit to the Arrhenius equation,

$$\sigma T = B \exp\left(-\frac{E_a}{k_B T}\right) \qquad (1)$$

where, B is an exponential factor, E_a the activation energy, k_B the Boltzmann constant, and T the absolute temperature, has been made in this temperature range. The fitted lines are shown in Fig. 2. An advantage of fitting the data to the Arrhenius equation is the possibility of calculating E_a values whose physical meaning is, however, not clear. The activation energy values extracted from this equation are shown in Fig. 3. The high conductivity samples show low E_a values and vice versa as expected.

As for many polymer electrolytes, there is a distinct hysteresis observed for the conductivity behavior in this case. There are evidences of hysteresis enhancing the conductivity of the electrolyte samples after annealing. Conductivity measurements, taken after annealing the samples to 100 °C (above T_m), seem to follow the trend
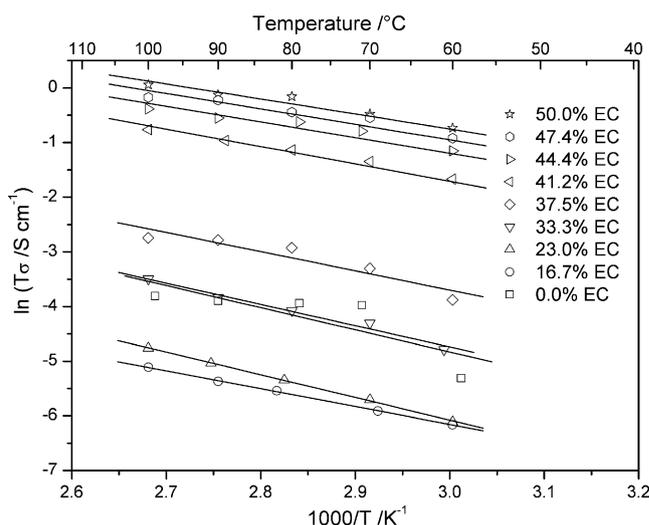
Fig. 2 The conductivity versus 1,000/T with fitted straight lines for (PEO)$_{68}$Pr4N$^+$I$^-$/I$_2$/EC electrolytes containing different mass fractions of EC at temperatures above 60 °C
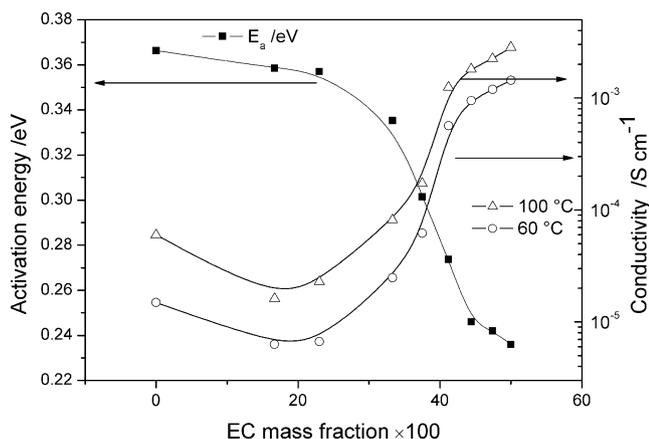
Fig. 3 Activation energy for the temperature range 60–100 °C and conductivity at 60 and 100 °C versus EC mass fraction for the polymer electrolyte, $(PEO)_{68}Pr4N^+I^-/I_2/EC$

of the high temperature (above 60 °C) measurements even at low temperatures, resulting in a conductivity of 1.5×10^{-4} S cm^{-1} at 0 °C even after 24 h, see the inset in Fig. 1. However with prolonged aging of the annealed electrolyte samples, the low-temperature conductivity drops gradually, and the abrupt conductivity increase at the melting temperature reappears. The dielectric parameters also change in a similar manner after annealing the samples.

According to Figs. 1 and 3, the conductivity of all the plasticized electrolyte samples increases with the EC content. This is to be expected due to the increased salt dissociation and increased ionic mobility caused by the plasticizer. At temperatures below the PEO crystallite melting temperature, T_m, the conductivity increase is due to the reduction of crystallinity of PEO and associated structural and morphological changes of the electrolyte brought about by the plasticizer [2]. In addition, the EC plasticizer also undergoes melting around 35 °C and starts to contribute toward enhancing the conductivity through increased mobility and ionic dissociation, and this contribution appears to be significant for higher EC concentrations.

At temperatures above T_m, both the amorphous phase of PEO and the presence of the EC plasticizer would contribute to the overall conductivity. It may be noted that, at these temperatures, the unplasticized sample shows somewhat higher conductivity compared to the two plasticized samples with lowest EC contents. In these low EC content samples, there is the possibility that localized, isolated EC-rich regions with dissolved ions may exist, thereby depleting the ionic concentration in the host PEO matrix. This situation can be expected, as the EC plasticizer is more polar in nature compared to the PEO. These EC rich regions, however, may not contribute to the overall conductivity due to their localized and isolated nature. This could be the reason for the low EC content samples to show

a lower conductivity compared to that of the unplasticized samples at higher temperatures.

DSC measurements were used to determine the melting temperature (T_m) and the glass transition temperature (T_g) for the prepared electrolyte samples, see Fig. 4. One endothermic peak at about ~60 °C is observed for all the electrolyte samples. This is evidently associated with the melting of PEO crystallites. For samples with higher EC mass fractions, an additional peak appears. The temperature of this peak ranges from 14.4 °C for the 28.6 % EC sample to 28.8 °C for the 50.0% EC sample. We may conclude that this low temperature peak is related to the melting of the EC-rich phase in the electrolyte sample. The peak at 66.1 °C for the unplasticized sample shifts to lower temperatures when plasticizer is introduced and occurs at 45.2 °C for the samples with 50% EC. The two melting peaks that correspond to the melting of the PEO crystallites and the melting of the EC-rich phase appears to merge for EC mass fraction above 50%. At these high EC concentrations, the broad nature of the double peak makes it difficult to identify the individual peak temperatures. For comparison, the melting peak of pure EC is also shown in Fig. 4. The glass transition was observed for all samples; see the inset in Fig. 4 and Table 1. The T_g values decrease with the mass fraction of plasticizer as expected, from −57.6 °C for the unplasticized sample to −70.92 °C for the 50% EC sample. Decreasing T_g values can also be correlated with the corresponding increase in conductivity, since the segmental motion of the host polymer matrix is important for the conductivity [2, 7, 17, 18]. The rapid conductivity increase
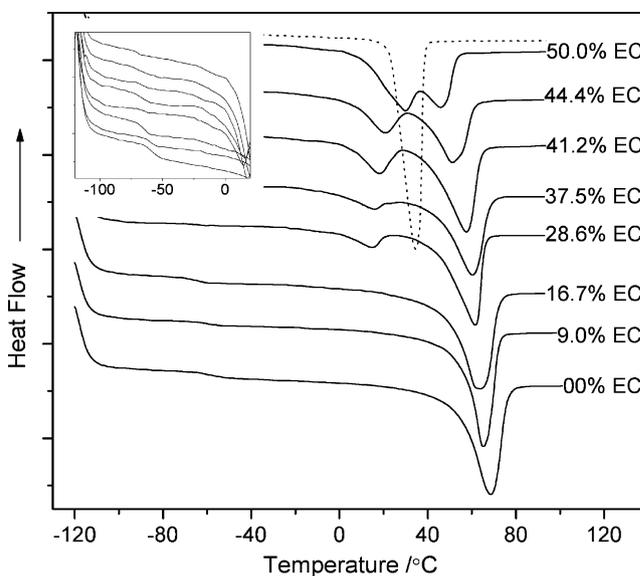
Fig. 4 DSC thermograms of the $(PEO)_{68}Pr4N^+I^-/I_2/EC$ polymer electrolyte samples for different EC mass fractions. The *dotted line* shows the DSC thermogram for pure EC. The *inset* shows an enlargement of the glass transition region

Table 1 Glass transition temperature, T_g, and melting temperature, T_m, for different EC content for polymer electrolyte $(PEO)_{68}Pr4N^+I^-/I_2/EC$

EC mass fraction×100	$T_g/°C$	$T_m/°C$ (peak 1)		$T_m/°C$ (peak 2)	
		Peak	Onset	Peak	Onset
0	−57.6	66.1	57.7	–	–
9.0	−59.6	63.7	56.0	–	–
16.7	−63.9	63.1	49.2	–	–
28.6	−64.3	60.7	43.6	14.4	1.4
37.5	−65.9	59.4	43.5	15.0	2.0
41.2	−67.7	56.7	39.6	17.4	5.4
44.4	−68.5	52.6	38.1	18.0	6.4
50.0	−70.9	45.1	37.7	28.8	14.0

Fig. 5 ε' versus frequency for the electrolyte sample $(PEO)_{68}Pr4N^+I^-/I_2$ with 20% EC mass fraction at different temperatures

and the associated decrease in activation energy shown in Fig. 3 can be attributed to the development of the low-temperature melting peak shown in the DSC traces in Fig. 4. The corresponding EC-rich phase is evidently more favorable for ionic migration [16, 19].

High-frequency dielectric measurements may provide an efficient approach to probe the interactions taking place in the electrolyte [20, 21]. The complex dielectric constant $\varepsilon^*(\omega, T) = \varepsilon'(\omega, T) - j\varepsilon''(\omega, T)$ can be obtained from the real and imaginary parts of the complex impedance Z' and Z'',

$$\varepsilon' = -\frac{dZ''}{\omega\varepsilon_o A(Z'^2 + Z''^2)} \qquad (2)$$

$$\varepsilon'' = \frac{dZ'}{\omega\varepsilon_o A(Z'^2 + Z''^2)} \qquad (3)$$

where A is the cross section area and d the thickness of the sample, and ε_o the permittivity of vacuum and $j^2 = -1$. ε'' is strongly influenced by the high ionic conductivity in the electrolyte samples, and a corrected ε'' value is calculated by subtracting the DC conductivity contribution ($\sigma/\varepsilon_o\omega$) from the total ε'' value obtained from Eq. 3. Dielectric data can be used to detect relaxation of electric dipoles, permanent or induced. A relaxation is shown as a step in ε' and a peak in ε''. Relaxation peaks due to ion pair dipoles has, for example, been detected for other polymer electrolyte systems and may be related to the local viscosity and the ionic mobility in the electrolyte [18, 20].

The frequency dependence of the real part of the dielectric constant (ε') for the polymer electrolyte with different amounts of EC was measured in the frequency range 1 MHz to 1 GHz for samples containing 0–50 wt.% EC; a typical set of data is shown in Fig. 5. The high frequency plateau values here denoted by ε'_S are shown in Fig. 6 as a function of temperature and EC content. ε'_S

increases with the amount of EC, an expected result since ε' for pure EC is 89.8 [2] while ε' for pure PEO is about 5 at 23 °C. The ε'_S values increase with the mass fraction of plasticizer, from 3.3 for the unplasticized sample to 17.5 for the 50% EC sample. A marked increase of ε' can be observed when the temperature reaches the melting temperature of the PEO-rich phase. The variation of the onset of the PEO melting peak shown in Fig. 4 and Table 1 appears to correlate well with the onset of the increase of ε'_S values shown in Fig. 6. In general, an increase in the dielectric constant is expected to be associated with an increasing ionic conductivity due to its effect on ionic dissociation. Such a general trend can be observed in Fig. 6, although it is not followed in detail. Of course, the ion dissociation is not the only effect influencing ionic conductivity. For example, the ionic mobility is also related to the glass transition temperature, as discussed above.
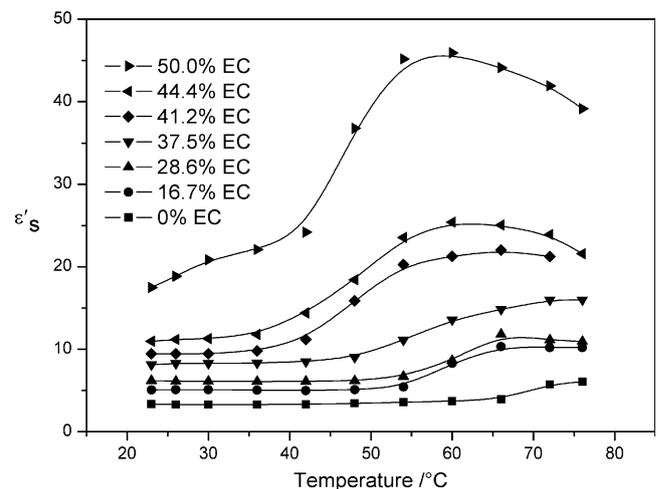
Fig. 6 ε'_s plateau value versus temperature for $(PEO)_{68}Pr4N^+I^-/I_2$ electrolytes with different amount of EC

For this type of electrolytes, a number of dielectric relaxations may be detected due to, for example, polymer and ion–ion dipoles. Calculating the corrected imaginary part of the dielectric constant for these electrolyte samples is difficult due to the high ionic conductivity. However, from our results (not shown), only a small relaxation peak in the low-frequency part might be observed. This is most probably related to a high degree of ionic dissociation, leaving out only small traces of ion-pair relaxations. We may thus conclude that the iodide ion is well dissociated and, despite its large size, is an efficient charge carrier giving rise to relatively high conductivity even though the iodide ion to ether oxygen ratio is as low as 1:68 in these samples.

Conclusion

The conductivity of the plasticized, iodide-ion-conducting electrolyte $(PEO)_{68}Pr_4N^+I^-/I_2/EC$ can reach values of 9.5×10^{-5} S cm^{-1} at room temperature, increasing to 1.4×10^{-3} S cm^{-1} at 60 °C, which is not an unusual temperature for an operating solar cell. The activation energy values measured above the polymer melting temperature decreases from 0.37 to 0.24 eV when the mass fraction of EC increases from 0% to 50%. A significant contribution to the observed conductivity enhancement in the PEO-based polymer electrolyte appears to come from the EC-rich phase. The formation and the development of this phase is clearly visible in the DSC thermograms as an additional first-order phase transition. This melting peak starts to appear when the EC mass fraction is 28.6%. The static dielectric constant of the electrolyte, which gives a measure of the polarizability of the material, increases with the amount of plasticizer and the temperature. Dielectric data show that ion association is low in these samples, contributing to high iodide ion conductivity. This type of electrolyte could thus be a suitable candidate for PEC solar cells, although a further enhancement in ionic conductivity, especially at the lowest temperatures, is desired.

References

1. Ritchie AG (2004) J Power Sources 136:285–289 doi:10.1016/j.jpowsour.2004.03.013
2. Stephan AM (2006) Eur Polym J 42:21–42 doi:10.1016/j.eurpolymj.2006.02.006
3. Dissanayake MAKL, Jayathilaka PARD, Bokalawala RSP, Albinsson I, Mellander B-E (2003) J Power Sources 119–121:409–414 doi:10.1016/S0378-7753(03)00262-3
4. Kim KH, Kang M, Kim YJ, Won J, Park N, Kang YS (2004) Chem Commun (Camb) 14:1662–1663 doi:10.1039/b405215c
5. Grätzel M (2003) J Photochem Photobiol Chem 4:145–153 doi:10.1016/S1389-5567(03)00026-1
6. Ileperuma OA, Dissanayake MAKL, Somasunderam S, Bandara LRAK (2004) J Sol Energy Mater Sol Cells 84:117 doi:10.1016/j.solmat.2004.02.040
7. Volel M, Armand M (2004) Macromolecules 37:8373–8380 doi:10.1021/ma0490404
8. Bandara TMWJ, Dissanayake MAKL, Ileperuma OA, Varaprathan K, Vignarooban K, Mellander B-E (2007) J Solid State Electrochem 12:913–917. doi:10.1007/s10008-007-0461-7
9. Tennakone K, Senadeera GKR, Perera VPS, Kottegoda IRM, Silva LAAD (1999) J Chem Mater 11:2474 doi:10.1021/cm990165a
10. Dissanayake MAKL, Bandara LRAK, Bokalawala RSP, Jayathilaka PARD, Ileperuma OA, Somasunderam S (2002) Mater Res Bull 37:867 doi:10.1016/S0025-5408(02)00712-2
11. Lan Z, Wu J, Lin J, Huang M, Li P, Li Q (2008) Electrochim Acta 53:2296–2301 doi:10.1016/j.electacta.2007.09.061
12. Huo Z, Dai S, Wang K, Kong F, Zhang C, Pan X et al (2007) Sol Energy Mater Sol Cells 91:1959–1965 doi:10.1016/j.solmat.2007.08.003
13. Xue B, Wang H, Hu YS, Li H, Wang ZX, Meng QB et al (2004) Photochem Photobiol Sci 3:918 doi:10.1039/b412647e
14. Wang G, Zhou X, Li M, Zhang J, Kang J, Lin Y et al (2004) Mater Res Bull 39:2113–2118 doi:10.1016/j.materresbull.2004.07.004
15. Wang XJ, Zhang HP, Kang JJ, Wu YP, Fang SB (2006) J Solid State Electrochem 11:21–26 doi:10.1007/s10008-005-0029-3
16. Berthier C, Gorecki W, Minier M, Armand MB, Chabagno JN, Rigaud P (1983) Solid State Ion 11:91–95 doi:10.1016/0167-2738(83)90068-1
17. Mellander B-E, Albinsson I (1996) New Developments. In: Chowdari BVR (ed), Solid State Ionics, World Scientific Publishing Co. P. 83-95 and 97-115
18. Jayathilaka PARD, Dissanayake MAKL, Albinsson I, Mellander B-E (2003) Solid State Ion 156:179–195 doi:10.1016/S0167-2738(02)00616-1
19. Tunstall DP, Tomlin AS, Gray FM, MaccCallum JR, Vincent CA (1989) J Phys Condens Matter 1:4035–4045 doi:10.1088/0953-8984/1/26/001
20. Mellander B-E, Albinsson I, Stevens JR (1994) Solid State Ion 72:177 doi:10.1016/0167-2738(94)90144-9
21. Ramesh S, Yahaya AH, Arof AK (2002) Solid State Ion 152:291–294 doi:10.1016/S0167-2738(02)00311-9